

Monte Carlo simulation of topological defects in the nematic liquid crystal matrix around a spherical colloid particle

R. W. Ruhwandl and E. M. Terentjev

Cavendish Laboratory, University of Cambridge, Madingley Road, Cambridge CB3 0HE, United Kingdom

(Received 24 March 1997)

We use a Monte Carlo algorithm to simulate the director field around a spherical inclusion in a uniform nematic liquid crystal matrix. The resulting structure crucially depends on the relative strength of the nematic bulk elasticity and the director anchoring on the particle surface. When this anchoring is weak, the director field perturbations are small and have quadrupolar symmetry. With increasing strength of anchoring two topologically nontrivial situations are possible: a dipolar configuration with a satellite point defect (hedgehog) near the particle pole, or a quadrupolar configuration with a ‘‘Saturn ring’’ of disclination around the particle equator. [S1063-651X(97)01311-1]

PACS number(s): 61.30.Jf, 61.30.Gd, 64.70.Md, 61.20.Ja

I. INTRODUCTION

The problem of colloid particles introduced into a nematic liquid crystal matrix has recently attracted attention and has produced different views on the problem. A closed inner surface with sufficiently strong anchoring creates a topological mismatch of the director field $\hat{\mathbf{n}}$ between the director on the particle surface and the uniform director at large distances. This mismatch leads to topological defects, i.e., regions where the liquid crystal order and the continuity of $\hat{\mathbf{n}}(\mathbf{r})$ break down. A connected closed surface with homeotropic boundary conditions (the molecules and, therefore, the director $\hat{\mathbf{n}}$ are locked perpendicular to the surface) represents a point topological charge $N=1$. Since the overall sample with a uniform far field (i.e., $\hat{\mathbf{n}}$ is constant at a distant outer surface) has the topological charge $N=0$, the charge produced by the inner surface must be balanced by an additional opposite charge. There are two basic possibilities. The assumption that a spherical particle in a nematic represents a quadrupolar symmetry means that the director field should then be quadrupolar as well [1,2]. Hence the topological mismatch is balanced by a loop of a disclination with linear strength $m=-1/2$ and overall point charge $N=-1$ in the equatorial plane of the particle [a ‘‘Saturn ring,’’ see Fig. 1(b)]. The other possibility is a dipolar configuration with a satellite point defect with $N=-1$ near one of the particle poles, recently proposed in [3], see Fig. 1(c). Both situations are supported by good theoretical arguments and here we shall employ Monte Carlo simulations to examine the advantages and disadvantages of both structures.

The conclusion of this work is that both structures are possible. Which configuration finally forms is to a large extent determined by the early formation or cooling process. Once one of the configurations is realized, it remains quite stable. The theoretical comparison of the energy of both states critically depends on the core energies of the disclination ring and the point defect. In the simulation it could only be very crudely accounted for and further investigations are needed to get a better estimate.

The article is organized as follows. The next section describes the key theoretical points behind this problem, in-

cluding the main equations used for the simulations. Section III describes the numerical method of simulated annealing, which we used in the computation. Section IV presents the results of the calculations and a critical discussion of their interpretation. In the final Sec. V we conclude the work and describe possible experiments.

II. BASIC CONCEPT

Nematic liquid crystals can be described on the continuum level by a director field $\hat{\mathbf{n}}(\mathbf{r})$ which is the average direction of a small sample of molecules around the point \mathbf{r} . Since $\hat{\mathbf{n}}$ represents only a direction, the modulus is fixed, $\hat{\mathbf{n}}^2=1$. The inversion of a nematic molecule does not change its physical properties. This fact is reflected in the further symmetry requirement $\hat{\mathbf{n}}=-\hat{\mathbf{n}}$, which makes nematics different from a simple vector-field system.

Provided that changes in the director field are on a much larger length scale than the molecular size, the free energy

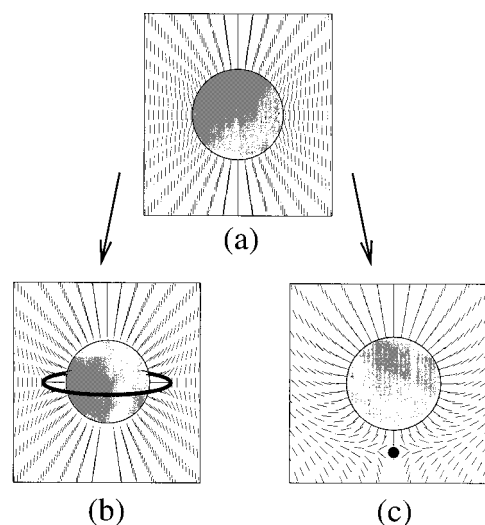


FIG. 1. (a) The director field in the case of weak anchoring. As the effective anchoring strength increases, there are two possibilities: the liquid crystal can form a quadrupolar Saturn ring structure (b) or a dipolar structure with a satellite defect (c).

density f_d due to bulk elastic deformations of the nematic can be written down as

$$f_d = \frac{1}{2} K_1 (\nabla \cdot \hat{\mathbf{n}})^2 + \frac{1}{2} K_2 (\hat{\mathbf{n}} \cdot \nabla \times \hat{\mathbf{n}})^2 + \frac{1}{2} K_3 (\hat{\mathbf{n}} \times \nabla \times \hat{\mathbf{n}})^2, \quad (1)$$

where the Frank elastic constants K_1 , K_2 , and K_3 describe the energy increase due to splay, twist, and bend of the director, respectively. The three elastic constants are of the same order of magnitude in many practical cases and we employ the one-constant approximation of the Frank elastic energy,

$$f_d = \frac{1}{2} K [(\operatorname{div} \hat{\mathbf{n}})^2 + (\operatorname{curl} \hat{\mathbf{n}})^2]. \quad (2)$$

Let us note here that Eq. (2) is slightly different from the familiar $\frac{1}{2} K (\nabla \hat{\mathbf{n}})^2$, which is obtained by the integration by parts [4]. The presence of topological defects with their core surfaces and, as in our case, the particle itself, makes the surface terms emerging from this integration ambiguous—or at least not straightforward. We have chosen not to discuss the surfacelike elastic constants K_{24} and K_{13} , but strictly speaking, their contribution on the cores of topological defects should also be considered.

In the case of a spherical particle in a nematic, which is uniform far away from the object (aligned parallel to the \hat{z} axis), the director $\hat{\mathbf{n}}$ can be expressed more conveniently in terms of the angle it makes with the \hat{z} axis of the spherical coordinate system, $\beta(r, \phi, \theta)$, or rather $\beta(r, \theta)$ since there is an obvious azimuthal symmetry in the problem. We assume homeotropic boundary conditions where the director has to be perpendicular to the surface of the particle. A deviation from this ideal orientation is penalized by the surface energy [5]

$$\mathcal{F}_s = -\frac{1}{2} W \oint (\hat{\mathbf{n}} \cdot \hat{\mathbf{v}})^2 dS, \quad (3)$$

where $\hat{\mathbf{v}}$ is the surface normal and W is the anchoring energy. The relative strength of the director anchoring compared to the bulk elastic energy can be expressed by the dimensionless parameter WR/K , where R is a typical length scale of the problem (the radius of the particle).

In the regime of weak-anchoring conditions $WR/K \ll 1$, the bulk elasticity prevails and the director field is only slightly distorted from its uniform orientation and does not have any disclination or point defects [see Fig. 1(a)]. The texture can be calculated analytically [2] and the solution satisfying the boundary conditions, $\beta = (WR/4K)(R/r)^3 \sin 2\theta$, has the expected quadrupolar symmetry. In order to investigate the director field under stronger-anchoring conditions ($WR/K \gg 1$), when the surface enforces the topological defects, we employed a numerical Monte Carlo algorithm to calculate $\hat{\mathbf{n}}(\mathbf{r})$.

If there are defects present in the system, the bulk free energy density Eq. (1) becomes singular and the description in terms of a director field breaks down in the core region. The liquid crystal “melts” locally into the isotropic phase since this is energetically preferable to large director gradi-

ents. The volume integration to obtain the bulk free energy $\mathcal{F}_d = \int f_d dV$ from Eq. (1) does not extend over the volume of the disclination or the point defect core, but a certain core energy E_c has to be added to the free energy for this region (see further discussion of this issue in Sec. V).

III. NUMERICAL METHOD

During the last few decades Monte Carlo simulations have proven to be a powerful tool for the optimization of complex problems with a large number of degrees of freedom. In our case there is a certain number of grid points in space, which represent a discrete version of the director field, and at each of these points the director is described by the angle β . This angle can take arbitrary values between $-\pi/2$ and $\pi/2$, which makes it even theoretically impossible to calculate the free energy of all possible configurations.

We used the method of simulated annealing, which belongs to the class of Metropolis algorithms, to find the state of the lowest energy. Instead of comparing different configurations, one (arbitrary) director distribution is taken and the free energy \mathcal{F} calculated. A random point of the configuration is then selected, altered by a random amount $\Delta\beta$ and the energy difference between old and new configuration $\Delta\mathcal{F}$ calculated. If $\Delta\mathcal{F}$ is negative, i.e., the altered director field has a lower energy than the unaltered one, the move is accepted. If $\Delta\mathcal{F}$ is positive, i.e., the change of the director increases the energy, the move is not immediately discarded but accepted with a probability of $e^{-\gamma\Delta\mathcal{F}}$, where γ (an effective temperature) is a value to be fixed during the calculation. This procedure is inspired by the way a real liquid crystal reaches its thermal equilibrium. Starting from the isotropic phase, where the direction of the molecules is arbitrary, it is cooled down into the anisotropic liquid crystalline phase. This happens at finite temperatures where certain fluctuations are inherent in the system, depending on the temperature. Therefore states which do not have the lowest energy are allowed and their probability is given by the Boltzmann factor $e^{-\Delta\mathcal{F}/k_B T}$. The simulation scheme mimics this behavior and the factor γ is just an artificial inverse temperature. Without permitting the moves that increase the energy, the calculation would end up at the nearest local minimum instead of reaching the desired global equilibrium.

It is preferable to start using large changes of β at a high temperature and then to cool it gradually down to zero temperature. It must be emphasized that the “temperature” in this calculation scheme has no real physical meaning. The director is independent of any real temperature; any such dependence is contained in the order parameter of the system $Q = Q(T)$.

To reflect the azimuthal symmetry of the problem in the calculation, we transformed Eq. (1) into spherical coordinates, which then becomes independent of the azimuthal angle ϕ . Furthermore, an inverted radius $\xi = 1/r$ was used. This has two advantages: first, it enables the use of boundary conditions at infinity (points with $\xi = 0$). Secondly, in the discretized form, it produces a high density of grid points close to the particle surface, where most of the director changes occur and few grid points far from the particle, where the director variations are less relevant.

The free energy derived from Eq. (1) depends on the

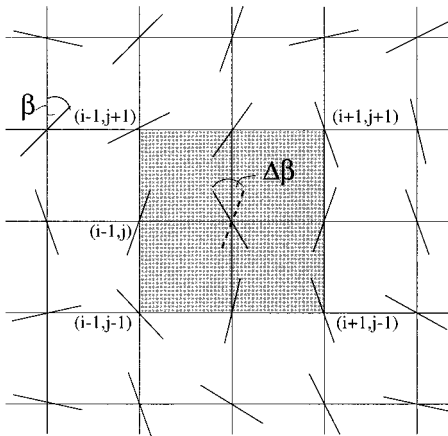


FIG. 2. The four surrounding meshes are used to calculate the change in the free energy after varying the director at point (i,j) by the amount $\Delta\beta$.

angle β and on its first derivatives with respect to ξ and θ . Since the derivatives are calculated by the nearest neighbors, there is no need to evaluate the energy in the whole system after each iteration. It is sufficient to calculate the energy only in the region where it is altered by the change of the director. Some care is necessary since every symmetric formula to evaluate a derivative at point (ξ,θ) is independent of the value at this point. In order to avoid this problem, the four meshes surrounding the point in question were used to evaluate the free energy, where the angle in the center of a mesh was calculated by the average of the four angles surrounding this point (see Fig. 2).

Further care has to be taken when the difference between two directors is calculated. Due to the equivalence of the states $\hat{\mathbf{n}}$ and $-\hat{\mathbf{n}}$, in each azimuthal cross section, the angle β is the same as $\beta+k\pi$, where k is an integer. This has to be taken into account when other values are calculated. The angular difference between two neighboring directors must always be smaller than $\pi/2$. The same applies to the average of two neighboring directors. For example, the average of $-\pi/3$ and $\pi/3$ is not 0 but $\pi/2$.

The factor γ , which determines the fraction of accepted moves which increase the energy, was chosen to be small at the beginning of the run and then increased during run time. The maximum change for an angle in one step was chosen to be $\pm\pi/2$ at the beginning, when the field is random, and then decreased gradually, when the field was getting more and more ordered. The acceptance rate depends very much on these two values and there is no real rule how to choose them, but experience shows that the acceptance rate of moves in Monte Carlo simulations should be around 50% to obtain the best results.

The calculations were performed on a DEC Alpha 600 and a typical calculation with a grid size of 80×240 points needed several hours.

IV. RESULTS

The simulations showed that the director pattern has no single preferred configuration. Both satellite and ring structure [Figs. 1(b) and 1(c)] are possible outcomes of the simulation. Once their basic structure has evolved they remain

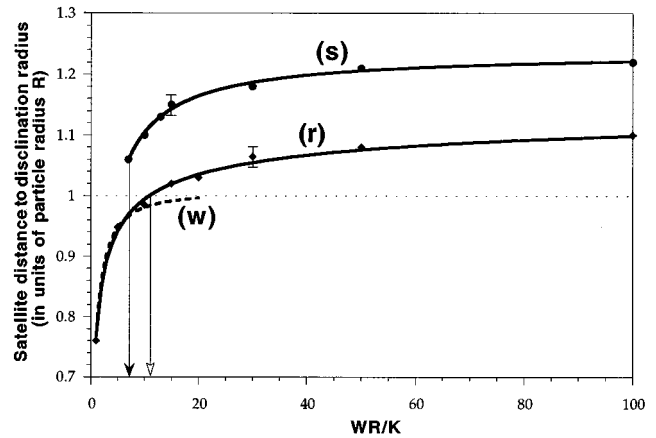


FIG. 3. The distance of the satellite from the center of the particle (curve s) and the radius of the disclination ring (curve r) and the virtual disclination inside the particle (curve w) in terms of the particle radius depending on the parameter $w=WR/K$. The error bars are slightly larger than the point distance of the grid.

stable with respect to the perturbations of the algorithm. This implies for the real system that the form of the director field is sensitive to the startup state. The stability of the two different solutions is also clearly the case in a real system. Even if the system has the Saturn ring texture whereas the satellite would be energetically favorable (or vice versa), the transition between the states is hardly possible. In order to shrink to a point defect, the disclination loop must move from the equatorial plane to one of the poles, but the intermediate stage of the ring, halfway up or down the particle, is energetically very costly, representing a high and wide barrier for the transition.

At the important transition region from strong to weak anchoring there is even a third class of solutions possible, the weak-anchoring distribution $\hat{\mathbf{n}}(\mathbf{r})$ without any topological defects, Fig. 1(a), along with the two main topologically non-trivial textures.

The distance a_s of the satellite defect from the center of the particle and the radius a_r of the disclination ring can act as order parameters of the transition from strong to weak anchoring. The equilibrium values of a_s and a_r were determined by running several simulations with the same parameter WR/K . There was usually no unique solution, i.e., the position of the defect and the radius of the disclination loop varied slightly. Therefore we plotted an energy vs distance curve and determined the equilibrium radius by taking the interpolated minimum of this curve. The error of this method is roughly given by the distance of two neighboring grid points, also because the exact location of the core is undetermined (it is "somewhere" between two grid points).

The variation of a_r and a_s with the control ratio WR/K is presented in Fig. 3. Figure 4 shows the energy of the three main configurations depending on the relative anchoring strength WR/K . The energy values obtained from the simulations were not continuous at the transition from weak to strong anchoring. This is not physical (the energy cannot jump) and the values were adjusted by adding a constant value to the energies of the satellite and the Saturn ring structure in such a way that there is a continuous increase in the energy. This has a physical reason: the free energy calculated

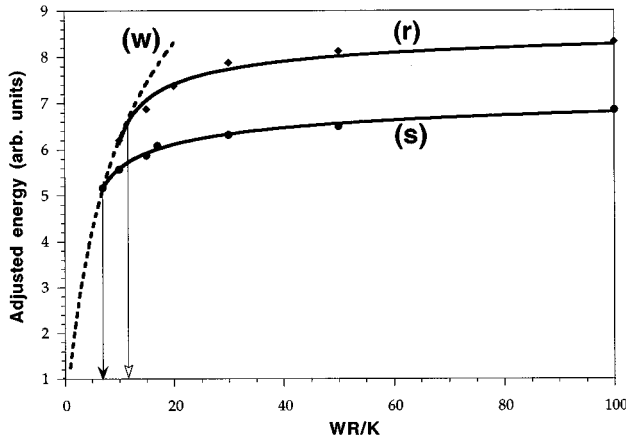


FIG. 4. The energies of the satellite (curve s) and Saturn ring fields (curve r) adjusted so that the transition from weak-anchoring texture (curve w) takes place without a jump in the free energy.

is merely the distortion free energy, i.e., the elastic energy of the bulk \mathcal{F}_d , and the anchoring energy at the particle surface \mathcal{F}_s , Eq. (3). There should be an additional term, the disclination core energy mentioned earlier, which could only be partly accounted for (see below). The simulation treats defect cores as a melted object of the size of a mesh with a homogeneous free energy density given by the values of the surrounding director. The idea is that it is preferable for the nematic liquid crystal to ‘melt’ rather than to sustain large director gradients. This does not really reflect the situation in real nematics, which is somewhat more complex and includes the coupling of the director $\hat{\mathbf{n}}$ with the order parameter distortions $\nabla\mathbf{Q}$ [6–8]. In the case of the satellite defect, a so-called hyperbolic monopole, the spherical symmetry disappears and it is even possible that a hedgehog does not really exist on a small length scale but it consists of a small disclination ring [9]. In summary, it is impossible to account for these subtle effects in the simulation framework we are using, which does not include the spatially varying order parameter.

The core region also introduces a new length scale (the core radius r_c) to the system, depending on the liquid crystal material constants. The satellite defect seems preferable for large particles since the Saturn ring changes its size with the particle radius. A straight disclination line (director field $n_x = \sin \phi/2$; $n_y = \cos \phi/2$; $n_z = 0$ for the defect line along the z axis) has the elastic energy per unit length of $E = K \ln r_o/r_c + \pi r_c^2 \varepsilon_c$ (see, for example, [10]), with r_o the outer cutoff radius and ε_c the core energy density, which leads for a ring of radius R to an energy estimate of $E_{\text{ring}} \propto 2\pi KR \ln R/\rho_c + 2\pi R(\pi\rho_c^2 \varepsilon_c)$ whereas for the satellite defect one roughly obtains $E_{\text{satellite}} \propto KR + E_{\text{core}}$ from considering a hedgehog point defect (director field $n_r = 1$; $n_\phi = n_\theta = 0$), with a size-independent total core energy $E_{\text{core}} = \frac{4}{3}\pi r_c^3 \varepsilon_c$. However, the relative value of the two core energy contributions is very difficult to estimate. For the line defect one has to balance the elastic energy density K/ρ_c^2 against the energy density of the melt, ε_c . This gives $\rho_c^2 \sim K/\varepsilon_c$ and the disclination core energy per unit length $\pi\rho_c^2 \varepsilon_c \sim \pi K$. On the other hand, for the point defect the similar argument would provide $E_{\text{core}} \sim \frac{4}{3}\pi K^{3/2} \varepsilon_c^{-1/2}$, not al-

lowing one to eliminate the poorly controlled thermodynamic energy density ε_c of an isotropic melt. An interested reader may refer to [7] for an additional discussion.

The core effects increase the energy of both the Saturn ring and the satellite structure. But they also affect the energy of the weak-anchoring field. When the ‘virtual’ disclination ring radius becomes of order R , a real disclination starts to appear at the surface of the sphere. Therefore the energy of this field (dashed line in Fig. 4) will also continuously increase to a higher value. Altogether it can be assumed that the effect of the defect core energy shifts the transition to a somewhat higher value of the control parameter $w = WR/K$.

The upper curve in Fig. 3, labeled (s), represents the distance of the satellite defect from the particle center, a_s/R . At $w \rightarrow \infty$ the distance of the satellite from the center has, according to the simulation, a value of $a_s \sim 1.22R$ which is somewhat larger than the estimate of [3]. On decreasing the effective anchoring it jumps at a critical value $w \sim 7$ from $a_s \sim 1.07R$ down to zero. For lower values there was no longer a minimum in the energy-distance plot, i.e., the satellite configuration becomes unstable and the weak-anchoring pattern favorable. At the same time the overall symmetry of the director field changes from the dipolar to quadrupolar. The jump in $a_s(w)$ and the clear break in the corresponding energy $\mathcal{F}(w)$ indicate that the transition is of first order. However, the phase transition from the satellite configuration to the weak-anchoring configuration undergoes a symmetry change from dipolar to quadrupolar, represented by the symmetry groups $D_{\infty h}$ and $C_{\infty h}$, respectively [11]. The order parameter of this transition can be easily identified: it is the z component p_z of a vector \mathbf{p} connecting the particle and the monopole. The expansion of the free energy in terms of the small order parameter cannot contain a cubic term p_z^3 (the free energy is a scalar, while p_z^3 changes sign on inversion). Therefore, from these underlying symmetry reasons, the transition seems to be of second order. One possibility to explain the jump in the order parameter and the break point in the energy curve at the absence of a cubic term in the Landau expansion of the free energy is to assume that the coefficient of the fourth-order term is negative and a sixth-order term has to be taken into account, i.e., the Landau expansion is of the form $\mathcal{F} = \frac{1}{2}a(w-w^*)p_z^2 - \frac{1}{4}bp_z^4 + \frac{1}{6}cp_z^6$.

The transition from a Saturn ring structure, the curve (r) in Fig. 3, seems to occur at a slightly higher value of the control parameter $w \sim 11$. At this point the combined curve of the satellite ring and the virtual disclination inside the particle has the value $a_r/R = 1$, i.e., the loop is on the surface of the sphere. The radius of the ring for infinite anchoring is slightly smaller than the estimate of [2], $a_r \sim 1.13$. Disclination radii of $a_r < 1$ do not represent real disclination rings but ‘virtual’ disclinations inside the particle. They were fitted using an approximate formula of the director field with a Saturn ring [2],

$$\beta = \theta - \frac{1}{2} \arctan \frac{\sin 2\theta}{(a_r/r)^3 + \cos 2\theta}. \quad (4)$$

The transition is continuous in the order parameter and in the free energy. This implies that the system undergoes a

second-order phase transition. Again, from symmetry arguments this cannot be the case: the transition from the Saturn ring is symmetry preserving. Both the ring and the weak anchoring $\hat{\mathbf{n}}(\mathbf{r})$ have quadrupolar symmetry and belong to the same group $D_{\infty h}$. It is a well known fact that phase transitions with preserved symmetry must be of first order (e.g., gas-liquid transition), which we do not see in our results. Therefore it seems that there is no phase transition as such. The disclination ring simply shrinks and, instead of being outside the sphere, a virtual ring continues to exist inside the sphere without any other changes in the system.

V. CONCLUSION

We examined the director structure around a spherical particle with a Monte Carlo simulation, depending on the anchoring energy of the nematic at the particle surface WR/K . In the region of strong-anchoring conditions ($WR/K \gg 10$) the director structure seems to depend on the history of the sample. If a preorder of quadrupolar structure existed, it will tend to remain in this symmetry and develop a Saturn ring texture. If this symmetry was not existent, but a dipolar prealignment configuration was enforced, the satellite structure will appear. Both patterns seem to be quite stable once they have formed and thermal fluctuations might not be strong enough to change the state to its global minimum, whatever it is, since the intermediate stage, a ring out of the equatorial plane, is punished by a high free energy. The question of which of the states has the lower energy cannot be answered unambiguously. Too little is known about the energy inherent in the core of a disclination ring or a monopole defect to be able to give a good estimate for the additional core energy. The scaling of the Saturn ring energy might imply that this structure is less favorable for large particles [3]. The conclusion that in the case of small particles the Saturn ring is preferable was also reached by Lubensky *et al.* [12]. The same holds of course for weak anchoring, for example, close to the melting point of a nematic liquid crystal where bubbles of isotropic material form inside the two-phase region.

The dipolar satellite defect texture would explain the alignment of particles in strings along the director lines observed in some experiments [3,13], whereas the quadrupolar structure would lead to repulsion along the director and attraction at oblique angles [14,15] leading to less structured aggregates also frequently observed [16]. On the other hand, the presence of other particles could distort the symmetry enough to favor the dipolar structure with a ring displaced from the equator and, therefore, explain the string alignment.

The simulations show a first-order phase transition from a satellite defect to the weak-anchoring field at $WR/K \sim 7$ or slightly higher. The transition from the Saturn ring to the weak-anchoring field occurs at somewhat higher values $WR/K \sim 11$. The disclination disappears from the liquid crystal but apparently continues to exist as a virtual ring inside the particle at any nonzero W . From symmetry arguments it can be conjectured that this change is not a real transition but rather a continuous process of decreasing $a_r(w)$.

The experimental examination of the director structure around a colloid particle with an optical microscope is difficult since samples with a reasonable thickness are turbid due to the high thermal fluctuations in nematics. An appropriate method of exploring even thick samples is the method of freeze fracturing or tomography. The sample is frozen and can be cut in thin slices in the region of interest to examine the director structure [17]. It is particularly interesting to examine the influence of the cooling method, cooling rates, and how symmetry breaking effects (such as the existence of other particles, electric and magnetic fields) change the director pattern.

ACKNOWLEDGMENTS

The authors have benefited from discussions with M. Warner, D. Lu, and P. D. Olmsted. We appreciate the chance given to us by the authors of [3] to see their paper prior to its publication. This research has been supported by EPSRC.

-
- [1] E. M. Terentjev, *Phys. Rev. E* **51**, 1330 (1995).
 - [2] O. V. Kuksenok, R. W. Ruhwandl, S. V. Shiyankovskii, and E. M. Terentjev, *Phys. Rev. E* **54**, 5198 (1996).
 - [3] P. Poulin, H. Stark, T. C. Lubensky, and D. A. Weitz, *Science* **275**, 1174 (1997).
 - [4] P. G. deGennes and J. Prost, *The Physics of Liquid Crystals*, 2nd ed. (Clarendon, Oxford, 1993).
 - [5] A. Rapini and M. Popolar, *J. Phys. (France)* **30**, 54 (1969).
 - [6] I. F. Lyuksyutov, *Zh. Eksp. Teor. Fiz.* **75**, 358 (1978) [*Sov. Phys. JETP* **48**, 178 (1978)].
 - [7] N. Schopol and T. J. Sluckin, *J. Phys. (France)* **49**, 1097 (1988).
 - [8] C. Chiccoli *et al.*, *J. Phys. (France) II* **5**, 427 (1995).
 - [9] H. Mori and H. Nakanishi, *J. Phys. Soc. Jpn.* **57**, 1281 (1988).
 - [10] M. Kléman, *Points, Lines and Walls* (John Wiley & Sons, Chichester, 1983).
 - [11] S. A. Pikin, *Structural Transformations in Liquid Crystals* (Gordon and Breach Publishers, New York, 1991).
 - [12] T. C. Lubensky, D. Petey, N. Courrier, and H. Stark, *cond-mat/9707133*.
 - [13] P. E. Cladis, M. Kléman, and P. Piéranski, *C. R. Acad. Sci.* **273**, 275 (1971).
 - [14] R. W. Ruhwandl and E. M. Terentjev, *Phys. Rev. E* **55**, 2958 (1997).
 - [15] S. Ramaswamy, R. Nityananda, V. A. Raghunathan, and J. Prost, *Mol. Cryst. Liq. Cryst.* **288**, 275 (1996).
 - [16] P. Poulin, V. A. Raghunathan, P. Richetti, and D. Roux, *J. Phys. II* **4**, 2497 (1995).
 - [17] Y. Bouligand, P. E. Cladis, L. Liebert, and L. Strzelecki, *Mol. Cryst. Liq. Cryst.* **25**, 233 (1974).